

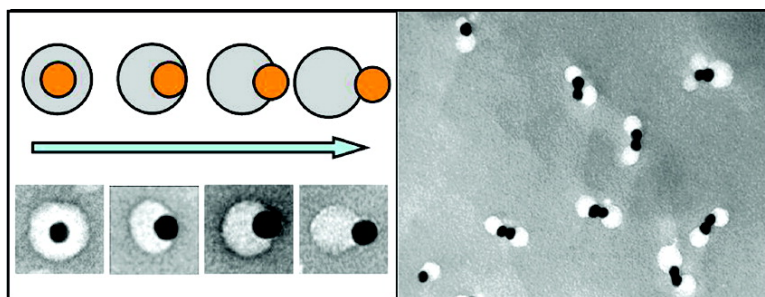
Communication

## Controlled Assembly of Eccentrically Encapsulated Gold Nanoparticles

Tao Chen, Miaoxin Yang, Xinjiao Wang, Li Huey Tan, and Hongyu Chen

*J. Am. Chem. Soc.*, **2008**, 130 (36), 11858-11859 • DOI: 10.1021/ja8040288 • Publication Date (Web): 16 August 2008

Downloaded from <http://pubs.acs.org> on February 8, 2009



### More About This Article

Additional resources and features associated with this article are available within the HTML version:

- Supporting Information
- Access to high resolution figures
- Links to articles and content related to this article
- Copyright permission to reproduce figures and/or text from this article

[View the Full Text HTML](#)

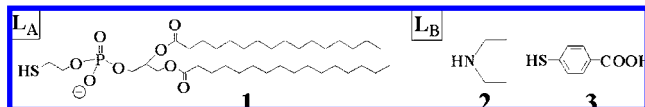
## Controlled Assembly of Eccentrically Encapsulated Gold Nanoparticles

Tao Chen, Miaoxin Yang, Xinjiao Wang, Li Huey Tan, and Hongyu Chen\*

Division of Chemistry and Biological Chemistry, Nanyang Technological University, Singapore 637371

Received May 29, 2008; E-mail: hongyuchen@ntu.edu.sg

Controlled functionalization of nanoparticle (NP) surface is of great importance in nanoscience. Due to the symmetrical shape and isotropic surface composition of NPs, however, it is difficult to attach molecules to a NP with defined stoichiometry. This has limited the effectiveness of using NPs as biolabels or as building blocks for a designed assembly. In the past few years, great efforts were made to break the symmetry of NP surface groups to allow specific functionalization. While many successes were reported on the preparation of micron-sized Janus (two-sided) particles,<sup>1</sup> the anisotropic functionalization of small NPs (<100 nm) remains a challenge. The most common preparative method utilizes interfacial surfaces to expose the diametric sides of a NP to different chemical environments, thus allowing selective activation of the surface groups.<sup>2</sup> Unfortunately, limited availability of interfacial surface often compromises the efficiency of this method. In addition, anisotropic NPs were prepared by controlling phase separation or surface nucleation of hybrid NPs.<sup>3</sup> Recently, specific functionalization of NPs with only a few reactive groups was also reported.<sup>4</sup>



Here we report a one-step, “mix-and-heat” synthesis for Janus NPs. It breaks the symmetry of surface functionalities on NPs by manipulating the core/shell structure of polymer-coated AuNPs (Figure 1). This control was realized by virtue of a binding competition between a hydrophobic ( $L_A$ ) and a hydrophilic ligand ( $L_B$ ) on the surface of AuNPs, which led to selective attachment of PS<sub>154</sub>-*b*-PAA<sub>60</sub> on one side of the AuNPs. Controlling the anisotropic polymer coverage opens up opportunities for selective functionalization and controlled assembly of the NPs.

Previously, homocentric core/shell AuNPs (Figure 1e, homo-[AuNP@polymer]) were prepared by reacting AuNPs with thiol-ended hydrophobic ligands (such as **1**) under conditions where amphiphilic diblock copolymers (such as PS<sub>154</sub>-*b*-PAA<sub>60</sub>) formed micelles.<sup>5</sup> The attachment of hydrophobic PS chains on the fully  $L_A$ -covered AuNP surface during self-assembly resulted in a uniform polymer layer. Introduction of an additional hydrophilic ligand ( $L_B$ ) during the encapsulation caused an intriguing change in the polymer attachment, giving NPs with eccentric core/shell structures (Figure 1f and 1g). Briefly, a mixture of citrate-stabilized AuNPs, PS<sub>154</sub>-*b*-PAA<sub>60</sub>,  $L_A$ , and  $L_B$  in DMF/H<sub>2</sub>O (volume ratio 4:1) was heated at 110 °C for 2 h and then slowly cooled down to induce polymer self-assembly. The synthesis can be easily scaled up to produce large quantities of ecc-[AuNP@polymer] uniform in size and morphology. The resulting NPs were readily purified by centrifugation; resuspension in water gave intact NPs free of reactants and empty micelles.

Deliberate addition of hydrophilic ligands such as diethylamine (**2**), 2-mercaptoacetic acid, or 4-mercaptopropionic acid (**3**) during

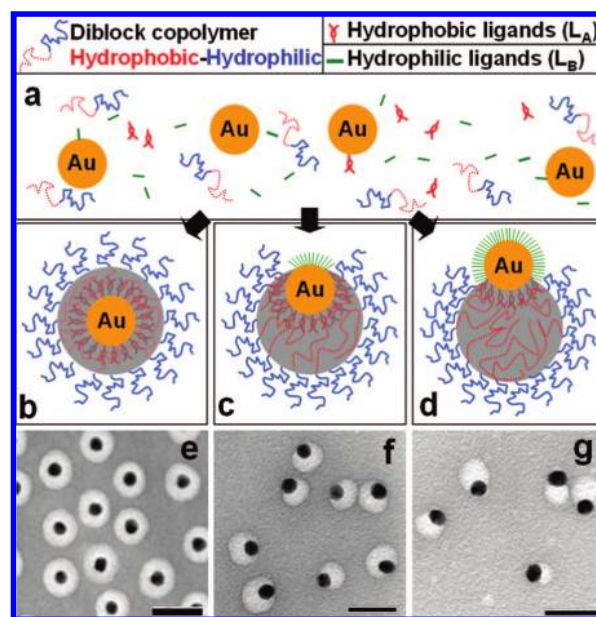


**Figure 1.** Schematic diagram showing the formation of homocentric (a and b) and eccentric (a, c, and d) AuNP@polymer. TEM images of purified AuNP@polymer when [1]:[2] = 1:0 (e); 1:22 (f); 1:132 (g), corresponding to b, c, and d, respectively. All scale bars are 50 nm.

the encapsulation all gave AuNP@polymer with an eccentric core/shell structure, indicating the key role of  $L_B$  in this process. Since surface-enhanced Raman scattering (SERS) signals of **3** were observed on the 40 nm ecc-[AuNP@polymer] (vide infra), we proposed that both  $L_A$  and  $L_B$  are coordinated to the AuNPs, with  $L_A$  embedded in the PS layer and  $L_B$  on the “exposed” surface of AuNPs as shown in the TEM images (Figure 1c, d). This assignment was supported by control experiments. Heating **1** with AuNPs in pure DMF without polymer gave a precipitate soluble in neither DMF nor water, suggesting that the  $L_A$ -coated surface is unstable in these solvents; encapsulation of AuNPs in the presence of  $L_B$  alone gave mainly free AuNPs unattached by polymer, suggesting that  $L_B$  is unstable inside the polymer shells. Therefore, the alternative assignment of  $L_A/L_B$  was ruled out.

The relative concentrations of  $L_A$  and  $L_B$  during encapsulation determine the morphology of AuNP@polymer. When [1]:[2] varied from 1:0, 1:22, to 1:132, the core/shell morphology evolved from homocentric (Figure 1e) to slightly eccentric (Figure 1f) and then to highly eccentric (Figure 1g). Apparently, the competition between **1** and **2** for surface binding sites has led to selective attachment of polymer on the partially  $L_A$ -covered AuNP surface. Increasing  $L_B$  concentration led to more competitive binding of  $L_B$  relative to the affinity of  $L_A$ , giving AuNP@polymer with a larger “exposed” surface. Polymer attachment further complicates the ligand competition by stabilizing  $L_A$  coordination. The  $L_A/L_B$  coverage ratios, as manifested from the ratio of the polymer-covered area to the

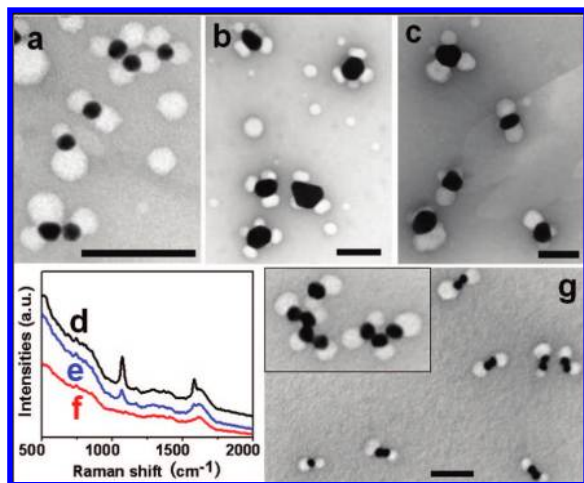


**Figure 2.** (a) TEM image of 15 nm AuNPs incubated with **2** followed by encapsulation with **1**; (b) TEM image of 40 nm AuNPs incubated with **3** followed by encapsulation with **1**, after purification. (c) TEM image of 40 nm AuNPs eccentrically encapsulated using **1** and **2**, purified, and then incubated with **3**. SERS signals of sample b (line d) and 40 nm AuNPs eccentrically encapsulated by **1** and **2** before (line f) and after (line e) incubation with **3**. (g) Aggregates of ecc-[AuNP@polymer], after incubation with basic NaCl solution (0.1 M NaCl and 0.04 M NaOH). All scale bars are 100 nm. See large-area views in the Supporting Information.

“exposed” area on each NP, are rather uniform (Figure 1f and 1g). Near-equilibrium conditions were seemingly attained during the eccentric encapsulation, as kinetically controlled ligand coordination/dissociation would have resulted in large differences of  $L_A/L_B$  coverage ratios on individual AuNPs.

Interestingly, when AuNPs were incubated with  $L_B$  prior to encapsulation with  $L_A$ , flower-like multiple micelle attachments on AuNPs were observed. The attachment number was generally 1–2 for 15 nm AuNPs (Figure 2a) and 3–5 for 40 nm AuNPs (Figure 2b and 2c), likely dictated by steric constraints. Specifically, the AuNPs were incubated with either **2** or **3** at room temperature for 2 h, followed by encapsulation in the presence of **1** (Figure 2c and 2b, respectively). SERS spectra of 40 nm AuNPs encapsulated using **1** and **3** (Figure 2d) showed the characteristic peaks of **3** at 1071 and 1576 cm<sup>-1</sup>,<sup>6</sup> confirming the presence of **3** near the Au surface. Preincubation with  $L_B$  was critical for this process. Randomly distributed, multiple micelle attachments on AuNPs were observed with the preincubation step, while uniform, single micelle attachment on AuNPs was observed without the preincubation step. These observations suggest that, with preincubation, the ligand dissociation and exchange were kinetically controlled, leading to uneven distribution of  $L_A$  on AuNPs. The irregularity in the number and size of the attached micelles in Figure 2a–c further supports this argument. This result, however, is in direct contrast with the uniform single-micelle-attached ecc-[AuNP@polymer] resulting from the free competition of  $L_A$  and  $L_B$  as discussed previously. A possible explanation for this paradox is that the incubation of AuNPs with  $L_B$  may have resulted in large patches of densely packed ligands that were kinetically difficult to displace; while under free competition, the transiently formed small patches of loosely packed ligands may undergo ligand exchange at near-equilibrium conditions. Previous studies have shown that a mixture of different thiol ligands coadsorbed on Au surface could result in phase segregation,<sup>7</sup> giving alternating patches of the ligands. The phase segregation is expected to be pronounced in our system, where two ligands with very

different hydrophilicity were used. The stabilization/destabilization effects from the polymer attachment could further encourage this segregation.

Selective functionalization of the nonsymmetrical AuNPs may open up opportunities for tailored NP organizations with novel properties. To test the exchangeability of  $L_B$  on the “exposed” AuNP surface, the flower-like ecc-[AuNP@polymer] samples ( $d_{\text{AuNP}} = 40$  nm) prepared using **1** and **2**, after purification, were incubated with **3**. Since neither **1** nor **2** gives observable SERS signals (Figure 2f), the appearance of **3** signals after incubation (Figure 2e) demonstrated that the weaker amine ligand on ecc-[AuNP@polymer] can be displaced by a stronger thiol ligand.

Indeed, organization of AuNPs can simply be achieved via salt-induced aggregation. Figure 2g shows the results of a purified ecc-[AuNP@polymer] sample treated with basic NaCl solution. Dimers of AuNPs accounted for ~40% of the aggregates observed, while the rest consisted of monomers and short linear chains. The preferential formation of dimers instead of sterically allowed trimers or tetramers could be related to the tendency of linear AuNP organization induced by salt treatment.<sup>8</sup> The unique partially attached polymer shells on AuNPs allowed aggregation but at the same time limited the size of the resulting aggregates.

In summary, a facile approach has been developed to break the symmetry of surface functionalities on AuNPs, where the core/shell arrangement of eccentric AuNP@polymer can be tuned utilizing the competitive coordination of the hydrophilic and hydrophobic ligands used in this system. Controlled aggregation of the resulting Janus NPs has been demonstrated. With more specific chemical functionalization, a wide range of AuNP organizations could be envisioned using the tunable nonsymmetrical core/shell structures.

**Acknowledgment.** The authors thank MOE (RG 52/07 and ARC 27/07) for financial support.

**Supporting Information Available:** Details for synthesis and characterization; large-area views of TEM images. This material is available free of charge via the Internet at <http://pubs.acs.org>.

## References

- Walther, A.; Muller, A. H. E. *Soft Matter* **2008**, *4*, 663–668. Perro, A.; Reculusa, S.; Ravaine, S.; Bourgeat-Lami, E.; Duguet, E. *J. Mater. Chem.* **2005**, *15*, 3745–3760.
- See: Lattuada, M.; Hatton, T. A. *J. Am. Chem. Soc.* **2007**, *129*, 12878–12889. Rycenga, M.; McLellan, J. M.; Xia, Y. N. *Adv. Mater.* **2008**, *20*, 2416–2420. Liu, X.; Worden, J. G.; Dai, Q.; Zou, J. H.; Wang, J. H.; Huo, Q. *Small* **2006**, *2*, 1126–1129. Xu, X.; Rosi, N. L.; Wang, Y.; Huo, F.; Mirkin, C. A. *J. Am. Chem. Soc.* **2006**, *128*, 9286–9287. Gu, H.; Yang, Z.; Gao, J.; Chang, C. K.; Xu, B. *J. Am. Chem. Soc.* **2005**, *127*, 34–35, and references therein.
- See: Yang, J.; Elim, H. I.; Zhang, Q.; Lee, J. Y.; Ji, W. *J. Am. Chem. Soc.* **2006**, *128*, 11921–11926. Giersig, M.; Ung, T.; Liz-Marzan, L. M.; Mulvaney, P. *Adv. Mater.* **1997**, *9*, 570–575. Yu, H.; Chen, M.; Rice, P. M.; Wang, S. X.; White, R. L.; Sun, S. *Nano Lett.* **2005**, *5*, 379–382. Glaser, N.; Adams, D. J.; Boker, A.; Krausch, G. *Langmuir* **2006**, *22*, 5227–5229, and references therein.
- DeVries, G. A.; Brunnbauer, M.; Hu, Y.; Jackson, A. M.; Long, B.; Neltner, B. T.; Uzun, O.; Wunsch, B. H.; Stellacci, F. *Science* **2007**, *315*, 358–361. Kruger, C. P.; Agarwal, S.; Greiner, A. *J. Mater. Chem.* **2008**, *130*, 2710–2711.
- Chen, H. Y.; Abraham, S.; Mendenhall, J.; Delamarre, S. C.; Smith, K.; Kim, I.; Batt, C. A. *ChemPhysChem* **2008**, *9*, 388–392. Kang, Y. J.; Taton, T. A. *Angew. Chem., Int. Ed.* **2005**, *44*, 409–412. Kim, B. S.; Qiu, J. M.; Wang, J. P.; Taton, T. A. *Nano Lett.* **2005**, *5*, 1987–1991.
- Orendorff, C. J.; Gole, A.; Sau, T. K.; Murphy, C. J. *Anal. Chem.* **2005**, *77*, 3261–3266.
- Love, J. C.; Estroff, L. A.; Kriebel, J. K.; Nuzzo, R. G.; Whitesides, G. M. *Chem. Rev.* **2005**, *105*, 1103–1170. Jackson, A. M.; Myerson, J. W.; Stellacci, F. *Nat. Mater.* **2004**, *3*, 330–336.
- Zhang, H.; Wang, D. Y. *Angew. Chem., Int. Ed.* **2008**, *47*, 3984–3987.

JA8040288